

Optimization of evaporative cooling towards a large number of Bose-Einstein condensed atoms

Makoto Yamashita,¹ Masato Koashi,² Tetsuya Mukai,¹ Masaharu Mitsunaga,³
Nobuyuki Imoto,^{1,2} and Takaaki Mukai¹

¹*NTT Basic Research Laboratories, NTT Corporation, 3-1, Morinosato Wakamiya, Atsugi-shi, Kanagawa 243-0198, Japan*

²*The Graduate University for Advanced Studies, Shonan Village, Hayama, Kanagawa 240-0193, Japan*

³*Kumamoto University, Faculty of Science, Department of Physics, 2-39-1, Kurokami, Kumamoto 860-8555, Japan*

(November 20, 2018)

We study the optimization of evaporative cooling in trapped bosonic atoms on the basis of quantum kinetic theory of a Bose gas. The optimized cooling trajectory for ^{87}Rb atoms indicates that the acceleration of evaporative cooling around the transition point of Bose-Einstein condensation is very effective against loss of trapped atoms caused by three-body recombination. The number of condensed atoms is largely enhanced by the optimization, more than two orders of magnitude in our present calculation using relevant experimental parameters, as compared with the typical value given by the conventional evaporative cooling where the frequency of radio-frequency magnetic field is swept exponentially. In addition to this optimized cooling, it is also shown that highly efficient evaporative cooling can be achieved by an initial exponential and then a rapid linear sweep of frequency.

Pacs. 03.75.Fi, 05.20.Dd, 32.80.Pj

I. INTRODUCTION

Evaporative cooling is an essential experimental technique in the recent demonstrations of Bose-Einstein condensation (BEC) with magnetically trapped atomic vapor [1,2,3,4,5]. This cooling method is based on both the selective removal of energetic atoms through evaporation and collisional rethermalizations among remaining atoms [6,7]. The successful utilization of interatomic elastic collisions makes evaporative cooling highly efficient. A real system, however, involves other atomic collisions, such as elastic collisions with background gas, inelastic collisions due to dipolar relaxation and three-body recombination processes. These undesirable collisions result in a loss of the trapped atoms and seriously reduce the effectiveness of evaporative cooling.

For alkali-metal atoms, such as ^{87}Rb and ^{23}Na , three-body recombination becomes a dominant loss mechanism during evaporative cooling [6], and limits the final number of condensed atoms, N_0 , in the experiments. It is known that ^{87}Rb atoms suffer much severer losses than ^{23}Na atoms due to their much large rate coefficient of three-body recombination process [8,9]. BEC experiments have clearly reflected this fact: the reported N_0 value in ^{87}Rb is 10^6 at most [10], while that in ^{23}Na is

up to 5×10^7 [11]. The small BEC of ^{87}Rb is a great disadvantage with respect to its future application as an “atom laser” [12] and has to be overcome.

In this paper, we report the theoretical optimization of evaporative cooling, focusing on BEC experiments with ^{87}Rb atoms. Several theoretical works have considered the optimization of evaporative cooling to increase the cooling efficiency [13,14,6]. Especially, Ref. [14] optimized the evaporative cooling in atomic hydrogen not only theoretically but also experimentally. However, these studies are based on kinetic theory of a classical gas which fails around the BEC transition point, and therefore don't give us any information on the number of condensed atoms produced by evaporative cooling. Our analysis is based on quantum kinetic theory of a Bose gas [15] and can provide quantitative results on the increase in the number of condensed atoms by optimizing the evaporative cooling. We optimize the temporal frequency sweep of the radio-frequency (rf) magnetic field under a fixed trapping potential by following the variational method developed by Sackett *et al.* for evaporative cooling in a classical gas system [13]. We show that an accelerated sweep of the rf-field frequency around the BEC transition point can largely enhance the final number of condensed atoms compared with conventional cooling with an exponential sweep of the frequency. It is also demonstrated that highly efficient evaporative cooling can be achieved by an initial exponential and then a rapid linear sweep of frequency. Our present results provide a useful guideline to experimentalists aiming to achieve large condensates in ^{87}Rb atoms.

II. KINETIC THEORY OF EVAPORATIVE COOLING

A. Thermodynamics of trapped bosonic atoms

We begin with a review of our theoretical formulation [15]. During evaporative cooling, a magnetic potential, $U(\mathbf{r})$, is truncated depending on the frequency of the applied rf-magnetic field. The thermalized distribution of noncondensed atoms in such a truncated potential is well approximated by the truncated Bose-Einstein distribution function such that

$$\tilde{f}(\mathbf{r}, p) = \frac{1}{\exp(\epsilon_p/k_B T)/\tilde{\xi}(\mathbf{r}) - 1} \Theta(\tilde{A}(\mathbf{r}) - \epsilon_p), \quad (1)$$

where T is the temperature, $\epsilon_p = p^2/2m$ is the kinetic energy of atoms with momentum p and mass m , and $\Theta(x)$ is a step function. In this paper, we add tilde to the notations of the quantities evaluated through this truncated distribution function. $\tilde{\xi}(\mathbf{r})$ denotes the local fugacity including mean-field potential energy; $\tilde{\xi}(\mathbf{r}) = \exp\{[\mu - U(\mathbf{r}) - 2v\tilde{n}(\mathbf{r})]/k_B T\}$, where μ is the chemical potential, $v = 4\pi a\hbar^2/m$ is the interaction strength of atoms in proportional to the s -wave scattering length a , and $\tilde{n}(\mathbf{r})$ is the density profile of atoms. The step function eliminates the momentum states whose kinetic energy exceeds the effective potential height $\tilde{A}(\mathbf{r}) = \epsilon_t - U(\mathbf{r}) - 2v\tilde{n}(\mathbf{r})$, where ϵ_t is the truncation energy of a magnetic potential. We calculate the density profile of atoms using this truncated distribution function in a self-consistent way such that

$$\tilde{n}(\mathbf{r}) = 4\pi\hbar^{-3} \int \tilde{f}(\mathbf{r}, p) p^2 dp, \quad (2)$$

and the internal energy density similarly as

$$\tilde{e}(\mathbf{r}) = 4\pi\hbar^{-3} \int \epsilon_p \tilde{f}(\mathbf{r}, p) p^2 dp + v\tilde{n}^2(\mathbf{r}) + U(\mathbf{r})\tilde{n}(\mathbf{r}). \quad (3)$$

The spatial integrations of these density functions give the total number of atoms, $\tilde{N} = \int \tilde{n}(\mathbf{r}) d\mathbf{r}$, and the total internal energy, $\tilde{E} = \int \tilde{e}(\mathbf{r}) d\mathbf{r}$ respectively.

After the BEC transition, the atom density in the condensed region is obtained by the sum of a condensate $n_0(\mathbf{r})$ and saturated noncondensed atoms \tilde{n}_n such that $\tilde{n}(\mathbf{r}) = n_0(\mathbf{r}) + \tilde{n}_n$. The condensate is described by the Thomas-Fermi distribution $n_0(\mathbf{r}) = n_p - U(\mathbf{r})/v$ with the peak density of the condensate at the center of potential n_p , while \tilde{n}_n is evaluated through the truncated Bose-Einstein distribution function with the condition $\tilde{\xi}(\mathbf{r}) = 1$.

B. Dynamics of evaporative cooling

The dynamics of trapped atoms during evaporative cooling is investigated on the basis of quantum kinetic theory of a Bose gas, developed previously by the present authors [15]. Trapped atoms are removed from the potential by not only evaporation but also undesirable collisions, as mentioned in the introduction. The change rates (i.e., loss rates) of the total number of atoms and the total internal energy are calculated respectively as the sum of the contributions of all processes such that,

$$\begin{aligned} \frac{d\tilde{N}}{dt} &= - \int \dot{n}_{\text{ev}}(\mathbf{r}) d\mathbf{r} \\ &\quad - \sum_{s=1}^3 G_s \int K_s(\mathbf{r}) [\tilde{n}(\mathbf{r})]^s d\mathbf{r} + \left(\frac{\partial \tilde{N}}{\partial \epsilon_t} \right)_{T, \mu} \dot{\epsilon}_t, \\ \frac{d\tilde{E}}{dt} &= - \int \dot{e}_{\text{ev}}(\mathbf{r}) d\mathbf{r} \\ &\quad - \sum_{s=1}^3 G_s \int K_s(\mathbf{r}) \tilde{e}(\mathbf{r}) [\tilde{n}(\mathbf{r})]^{s-1} d\mathbf{r} + \left(\frac{\partial \tilde{E}}{\partial \epsilon_t} \right)_{T, \mu} \dot{\epsilon}_t. \end{aligned} \quad (4)$$

The rates \dot{n}_{ev} and \dot{e}_{ev} denote the evaporation rates of density functions derived from a general collision integral of a Bose gas system [15,16]. The parameters G_1 , G_2 , and G_3 are the decay rate constants of trapped atoms due to the background gas collisions, dipolar relaxation, and three-body recombination, respectively. K_s represents the correlation function which describes the s -th order coherence of trapped atoms, and we assume the expressions of K_s for an ideal Bose gas system [17,8]. The terms proportional to the change rate of truncation energy, $\dot{\epsilon}_t = d\epsilon_t/dt$, give the contribution of extra atoms ‘‘spilled over’’ when ϵ_t changes continuously in the forced evaporative cooling [18,14]. The dynamics of the evaporative cooling including the loss of trapped atoms is described by the coupled differential equations in Eq. (4). In our theoretical framework based on truncated Bose-Einstein distribution function, all thermodynamic quantities are given as the complicated functions of three independent variables: temperature T , chemical potential μ , and truncation energy ϵ_t . We derive here the useful thermodynamic relations in terms of the change rates of these variables:

$$\begin{aligned} \frac{d\tilde{N}}{dt} &= \left(\frac{\partial \tilde{N}}{\partial T} \right)_{\mu, \epsilon_t} \dot{T} + \left(\frac{\partial \tilde{N}}{\partial \mu} \right)_{T, \epsilon_t} \dot{\mu} + \left(\frac{\partial \tilde{N}}{\partial \epsilon_t} \right)_{T, \mu} \dot{\epsilon}_t, \\ \frac{d\tilde{E}}{dt} &= \left(\frac{\partial \tilde{E}}{\partial T} \right)_{\mu, \epsilon_t} \dot{T} + \left(\frac{\partial \tilde{E}}{\partial \mu} \right)_{T, \epsilon_t} \dot{\mu} + \left(\frac{\partial \tilde{E}}{\partial \epsilon_t} \right)_{T, \mu} \dot{\epsilon}_t, \end{aligned} \quad (5)$$

where \dot{T} and $\dot{\mu}$ are the change rate of temperature and that of chemical potential respectively. Substituting these relations into Eq. (4), we clearly see that the terms proportional to $\dot{\epsilon}_t$ are canceled out and both \dot{T} and $\dot{\mu}$ are determined by three variables T , μ , and ϵ_t .

C. Optimization of cooling trajectory

The optimum cooling trajectory in the evaporative cooling process is obtained approximately by following the instantaneous optimization procedure investigated in Ref. [13]. We determine the optimized cooling trajectory so as to achieve the maximum increase in phase-space

density $\tilde{\rho}$ with the smallest decrease in the number of trapped atoms \tilde{N} . In the nonuniform gas system, the phase-space density is evaluated at the peak position and given by $\tilde{\rho} = \tilde{n}(\mathbf{0})\lambda^3$ with the thermal de Broglie wavelength $\lambda = h/\sqrt{2\pi mk_B T}$. At each time, we calculate the optimum truncation energy ϵ_t^* by maximizing the derivative, $-d(\ln \tilde{\rho})/d(\ln \tilde{N})$, which describes the efficiency of evaporative cooling [13,6]. We use a more useful form of this derivative rewritten in terms of change rates of temperature, chemical potential, and truncation energy as,

$$-\frac{d(\ln \tilde{\rho})}{d(\ln \tilde{N})} = -\frac{\left(\frac{\partial \tilde{\rho}}{\partial T}\right)_{\mu, \epsilon_t} \dot{T} + \left(\frac{\partial \tilde{\rho}}{\partial \mu}\right)_{T, \epsilon_t} \dot{\mu} + \left(\frac{\partial \tilde{\rho}}{\partial \epsilon_t}\right)_{T, \mu} \dot{\epsilon}_t}{\left(\frac{\partial \tilde{N}}{\partial T}\right)_{\mu, \epsilon_t} \dot{T} + \left(\frac{\partial \tilde{N}}{\partial \mu}\right)_{T, \epsilon_t} \dot{\mu} + \left(\frac{\partial \tilde{N}}{\partial \epsilon_t}\right)_{T, \mu} \dot{\epsilon}_t} \times \left(\frac{\tilde{N}}{\tilde{\rho}}\right). \quad (6)$$

In the optimized evaporative cooling, the truncation parameter $\eta = \epsilon_t/k_B T$ changes more slowly than the variables T , μ , and ϵ_t . We neglect the change rate of this truncation parameter, and consequently $\dot{\epsilon}_t$ is related to \dot{T} as $\dot{\epsilon}_t/\epsilon_t = \dot{T}/T$ in Eq. (6). The value of optimum truncation energy ϵ_t^* is given as a function of both temperature T and chemical potential μ . Substituting this ϵ_t^* into Eq. (4), we obtain the coupled differential equations describing the dynamics of the optimized evaporative cooling. The time-evolution calculations are carried out numerically by repeating a series of steps consisting of instantaneous optimization and dynamical short-time evolution of Eq. (4) with the temporal value of ϵ_t^* . Furthermore we assume quick rethermalization, where the system is always described by the truncated distribution function [15,7]. The obtained function $\epsilon_t^*(t)$ corresponds to the optimized sweeping function of the rf-field frequency.

In the next section, we will show the numerical results calculated by using relevant experimental parameters and discuss the experimental possibility of making large condensates in ^{87}Rb atoms.

III. NUMERICAL RESULTS AND DISCUSSIONS

A. Optimized evaporative cooling

In our numerical calculations, we employed parameters corresponding to the experiments performed at the University of Tokyo [19]. The cloverleaf magnetic trap with bias field B_0 , radial gradient B' , and axial curvature B'' was modeled by the magnetic field of Ioffe-Pritchard type such that $B(r, z) = \sqrt{(\alpha r)^2 + (\beta z^2 + B_0)^2}$, where $\alpha = \sqrt{B'^2 - B''B_0/2}$ and $\beta = B''/2$. We used the typical values adopted experimentally, such as $B_0 = 0.9$ G, $B' = 180$ G/cm, and $B'' = 170$ G/cm². The corresponding trapping frequencies are $\omega_r = 2\pi \times 171$ Hz in

the radial direction, and $\omega_z = 2\pi \times 11.8$ Hz in the axial direction. The collisional parameters for the trapped $F = 1, m_F = -1$ state were set as follows [8]: s -wave scattering length $a = 5.8$ nm, loss rate constants due to background gas collisions $G_1 = 0.01$ s⁻¹, dipolar relaxation $G_2 = 1.5 \times 10^{-16}$ cm³s⁻¹, and three-body recombination $G_3 = 4.3 \times 10^{-29}$ cm⁶s⁻¹. We chose the temperature $T = 150$ μK , the peak density $\tilde{n}(\mathbf{0}) = 4.0 \times 10^{11}$ cm⁻³, and the number of trapped atoms $\tilde{N} = 1.0 \times 10^9$ as the initial evaporative cooling conditions.

The exponential sweep of the rf-field frequency is usually adopted in BEC experiments [19]. We also performed calculations assuming that the frequency, ν , is swept exponentially from 35 to 0.67 MHz in 60 s as in Ref. [19]. The comparison between the different sweeps of rf-field frequency, optimized or exponential, will clarify the merit of the present optimization procedure.

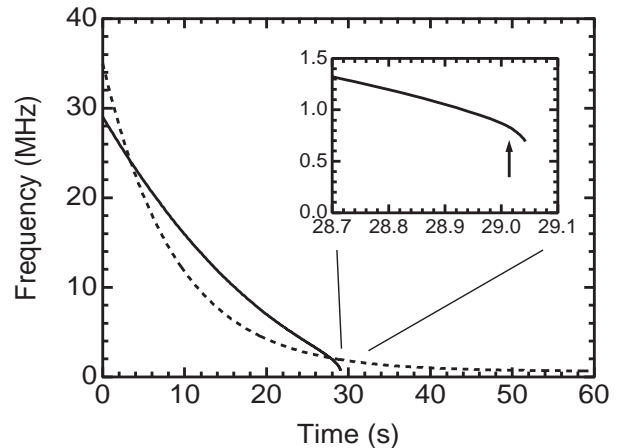


FIG. 1. Sweeps of rf-field frequency in the optimized case (solid) and in the exponential case (dashed). The inset shows the last part of the optimized sweep using an expanded scale. The arrow in the inset indicates the point at which the BEC transition occurs.

Figure 1 shows each sweep of the rf-field frequency. We see that the sweeping time (i.e., the cooling time) in the optimized case is about half that of exponential-sweep cooling for 60 s. The shorter sweeping time in the optimized cooling is advantageous for BEC experiments since the long time evaporative cooling easily becomes inefficient due to the instability of the magnetic trap. Furthermore, it is found that the optimized frequency sweep becomes rapid at the final stage of the cooling process, i.e., after about 27 s, and such a sweep is quite opposite to the exponential one which slows down over time. As shown in the inset of Fig. 1, the optimization procedure accelerates the evaporation around the BEC transition point. Similar acceleration of evaporation at the final stage of optimized cooling has been also demonstrated by the previous studies based on kinetic theory of a classical gas [13,14].

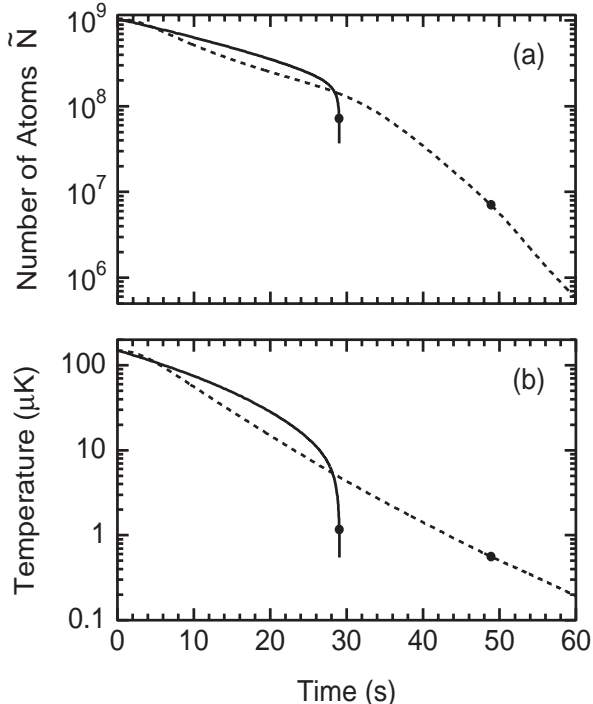


FIG. 2. Time evolution of (a) the total number of trapped atoms \tilde{N} and (b) temperature T , for optimized cooling (solid) and for exponential-sweep cooling (dashed). The dots indicate the points at which the BEC transition occurs.

In Figs. 2(a) and 2(b), we show the time evolution of the number of trapped atoms \tilde{N} and that of temperature T , respectively. In the optimized cooling, both \tilde{N} and T rapidly decrease at the final stage of cooling due to the rapid evaporation mentioned above. On the other hand, \tilde{N} and T decrease monotonically in the exponential cooling case. At the BEC transition point indicated by the dots in the figure, both the number of trapped atoms and temperature are calculated to be $\tilde{N} = 7.2 \times 10^7$ and $T = 1.2 \mu\text{K}$ at 29.01 s for the optimized cooling, and $\tilde{N} = 7.1 \times 10^6$ and $T = 0.56 \mu\text{K}$ at 48.9 s for the exponential cooling.

Next, we show how the optimization affects the cooling efficiency in the whole evaporative cooling process. In Fig. 3, the cooling trajectories of both cases are plotted in the \tilde{N} - $\tilde{\rho}$ plane and several corresponding time values are also added to the cooling trajectories to demonstrate the time evolution. At the early stage of cooling where the loss due to background gas collisions is dominant, both trajectories are quite similar, indicating that the exponential sweep of rf-field frequency is sufficiently good. However, the difference becomes larger as the trajectories approach the quantum degenerate region where the phase-space density exceeds the critical value of $\rho_c = 2.612$ and Bose statistics of atoms becomes dominant. Clearly, more atoms are lost in conventional

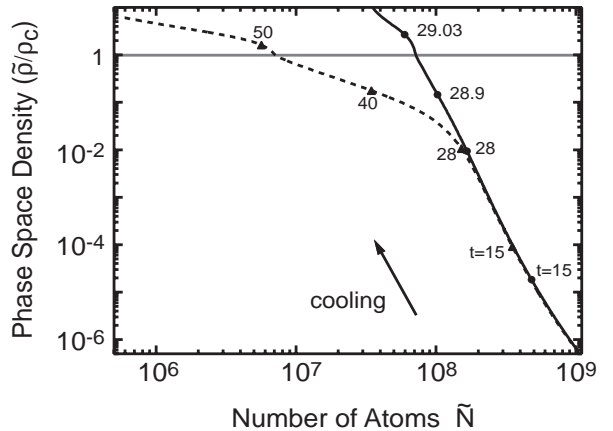


FIG. 3. Cooling trajectory through phase-space for optimized cooling (solid) and for exponential-sweep cooling (dashed). The phase-space density $\tilde{\rho}$ is normalized by the critical value $\rho_c = 2.612$. The BEC transition occurs when each trajectory passes the horizontal line where $\tilde{\rho}/\rho_c = 1$. The arrow indicates the direction of time. Several corresponding time values are added to the trajectories to demonstrate the time evolution of the system.

exponential-sweep cooling than in the optimized case. For example, we have ten times larger number of atoms in the optimized cooling at the BEC transition point when the trajectory reaches the horizontal line of $\tilde{\rho}/\rho_c = 1$. Note that the point where the two trajectories split up in Fig. 3 (i.e., $\tilde{\rho}/\rho_c \simeq 0.01$) corresponds to the time of around 28 s where the rf-field frequency curves cross in Fig. 1. The sudden increase in phase-space density just after the BEC transition in both trajectories reflects the rapid growth of condensate due to bosonic stimulation.

The number of condensed atoms, N_0 , is largely increased by the optimization. In the optimized cooling, N_0 increased monotonically and we obtained $N_0 = 2.1 \times 10^7$ after 29.04-s cooling. In the exponential-sweep cooling, on the other hand, N_0 had the maximum value of 1.74×10^5 at 57.0 s and then gradually decreased. We finally obtained $N_0 = 1.65 \times 10^5$ for 60-s exponential sweep cooling. More than a 100-fold enhancement of the number of condensed atoms was achieved in our present calculations. The lifetime of such a large condensate is evaluated to be less than 100 ms due to the enormous three-body recombination loss, as we will see in Fig. 4. However, it is possible to resolve this problem by adiabatically expanding the trapping potential. We also add that the value of $N_0 = 1.7 \times 10^5$ quantitatively agrees with the experimental results reported in Ref. [19] and confirms the validity of our numerical calculations.

The undesirable loss of trapped atoms during the cooling process gives us the physical origin of the rapid frequency sweep in the optimized cooling. Figure 4 shows the time evolution of loss rates of total number of trapped atoms at the final stage of the optimized cooling. It is

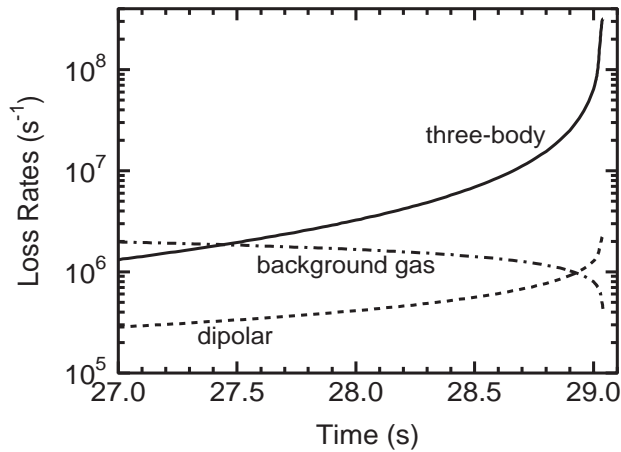


FIG. 4. Time evolution of loss rates at the final stage of optimized evaporative cooling, loss due to the background gas collision (dot-dashed), the dipolar relaxation process (dashed), and the three-body recombination process (solid).

seen that the loss due to the three-body recombination greatly increases and selectively removes atoms with high density (i.e., atoms with lower energy). This means that the serious heating of the system is caused by three-body recombination loss. In order to get a large number of condensed atoms, evaporative cooling should therefore be accelerated to compensate for such undesirable heating.

Here, we briefly discuss the validity of the quick rethermalization assumption in the rapid evaporation necessary for optimized cooling. The evolution of the system in the evaporative cooling process is well scaled by the characteristic time τ given by the inverse of normalized loss rate as $\tau = (-\dot{N}_{\text{loss}}/N)^{-1}$. The thermalization of the system, on the other hand, is characterized by the elastic collision time $\tau_{\text{coll}} = (n\sigma v)^{-1}$; n is the mean atom density, $\sigma = 8\pi a^2$ is the elastic collision cross section, and $v = 4\sqrt{k_B T/\pi m}$ is the mean velocity of relative motion of the atoms [20]. At the BEC transition point in the optimized cooling, these characteristic times are calculated to be $\tau = 140$ ms and $\tau_{\text{coll}} = 0.4$ ms, respectively. The relation $\tau \gg \tau_{\text{coll}}$ confirms that quick rethermalization is still valid during the rapid evaporation that occurs for optimized cooling.

B. Efficient evaporative cooling based on general sweeping functions of rf-frequency

The optimized frequency sweep in Fig. 1 is the complicated function of the experimental parameters such as the temperature, the density of gas, the atomic collisional parameters, the magnetic trapping potential, and so on. This means that we need to calculate the optimized cooling for each BEC experiment depending on its experimental conditions. Here we try to demonstrate the

efficient evaporative cooling based on general sweeping functions of rf-field frequency, which is useful for many experimentalists who want to achieve large condensates.

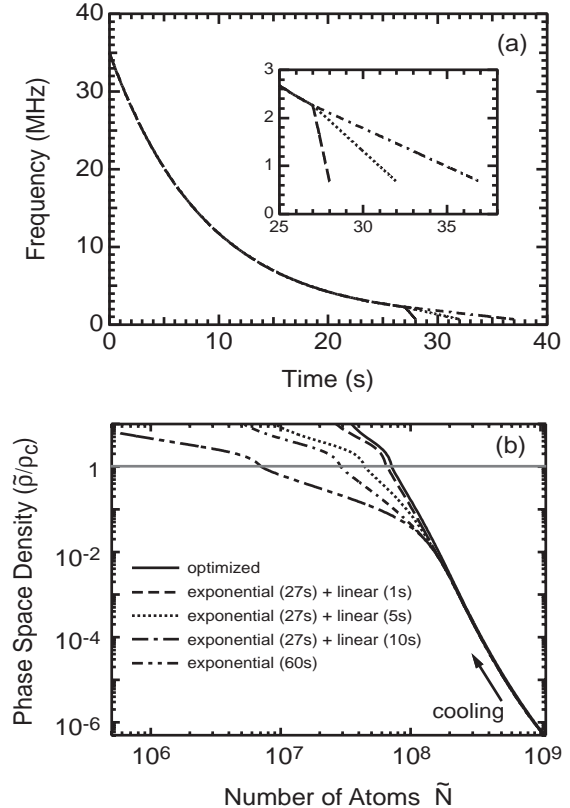


FIG. 5. (a) Sweeps of rf-field frequency consisting of two segments: an identical exponential sweep for 27 s and a sequential linear sweep for three different times which are 1, 5, and 10 s respectively. The exponential sweep is equal to the corresponding part of the dashed line in Fig. 1. The inset shows the linear-sweep region with an expanded scale. (b) Cooling trajectories through phase-space for the evaporative cooling using the sweeping functions in (a). The results of both optimized cooling and exponential cooling in Fig. 3 are also plotted for comparison. The phase-space density $\tilde{\rho}$ is normalized by the critical value $\rho_c = 2.612$. The BEC transition occurs when each trajectory passes the horizontal line where $\tilde{\rho}/\rho_c = 1$. The arrow indicates the direction of time.

From the results in Figs. 3 and 4, the exponential sweep is highly efficient until the three-body recombination loss becomes dominant. The rapid frequency sweep at the final stage of the optimized cooling in Fig. 1 might be approximated by a linear function. Thus it is expected that a combination of an exponential sweep of rf frequency and a rapid linear one realizes the high cooling efficiency. To test this cooling method, we carried out the time-evolution calculation by applying the same numerical parameters used in the optimization calculation of the preceding subsection. As shown in Fig. 5(a), the

frequency is first swept exponentially from 35 MHz to 2.26 MHz for 27 s and then swept linearly to 0.67 MHz for three different times of 1 s, 5 s, and 10 s respectively. The exponential curve in Fig. 5(a) is in conformity with the corresponding part of the dashed line in Fig. 1.

Figure 5(b) shows the cooling trajectories in the \tilde{N} - $\tilde{\rho}$ plane for the evaporative cooling using the sweeping functions of Fig. 5(a), together with those for the optimized and exponential cooling plotted in Fig. 3. We can see that the linear frequency sweep at the final stage of the evaporative cooling strongly improves the cooling efficiency as expected. Especially, the cooling trajectory in the case of 27-s exponential and 1-s linear frequency sweep (dashed line) is very close to the optimized one (solid line). The final number of condensed atoms in this cooling method is calculated to be $N_0 = 1.8 \times 10^7$ and comparable to the value in the optimized cooling such as $N_0 = 2.1 \times 10^7$. One can achieve the evaporative cooling with sufficiently high efficiency by an initial exponential and a sequential rapid linear sweep of rf-field frequency.

C. Experimental realization of efficient evaporative cooling

Recently, a group at Gakushuin University performed the efficient evaporative cooling for ^{87}Rb atoms with $F=2$, $m_F = 2$ trapped state [21]. They applied a frequency sweep similar to the optimized one which we calculated according to their experimental situations. The time of evaporative cooling was divided into three segments and in each segment the optimized sweeping function was approximated by the linear one: the frequency was swept linearly like $32 \rightarrow 13 \rightarrow 2 \rightarrow 1.1$ MHz for 10, 10, and 5 s respectively. A large number of condensed atoms, $N_0 = 1.4 \times 10^6$, were finally obtained after this 25-s evaporative cooling starting from the experimental conditions such as initial temperature $T = 380 \mu\text{K}$, initial total number of atoms $N = 4 \times 10^8$, and initial phase-space density $\rho = 5.8 \times 10^{-8}$.

On the other hand, we theoretically investigated this evaporative cooling. It was found that the cooling trajectory through phase space is close to that of optimized cooling and the final 5-s linear sweep of rf-frequency enhances the phase space density more than four orders of magnitude. The number of condensed atoms for this 25-s evaporative cooling was calculated to be 1.7×10^6 . Our calculated results agree well with the experiment at Gakushuin University.

IV. CONCLUSION

We have theoretically studied the optimization of evaporative cooling on the basis of quantum kinetic theory of a Bose gas, focusing on BEC experiments with rubidium

atoms. The calculated results indicate that the acceleration of evaporative cooling around the BEC transition point is very effective against serious three-body recombination loss. The number of condensed atoms is expected to be largely increased by this optimization procedure. Furthermore, it is shown that highly efficient evaporative cooling can be achieved by an initial exponential and then a rapid linear sweep of frequency. These results are consistent with the experiments and provide a useful guideline to experimentalists aiming to achieve large condensates in ^{87}Rb atoms.

In the present work, we optimized the sweeping function of the rf-field frequency only. A more complete optimization together with the adiabatic change of trapping potential curvature might produce a large and long-lived condensate. On the other hand, our theory neglects the influence of gravity which reduces the cooling efficiency at low temperatures [6]. An interesting future work would be to include the gravity in our present kinetic analysis and study how the optimized cooling trajectory is modified by it.

ACKNOWLEDGMENTS

We are grateful to Y. Yoshikawa, K. Araki, T. Kuwamoto, T. Hirano of Gakushuin University, M. Kozuma of the Tokyo Institute of Technology, T. Sugiyama, T. Kuga of the University of Tokyo, M. W. Jack and T. Hong of NTT Basic Research Laboratories for valuable discussions.

-
- [1] M. H. Anderson, J. R. Ensher, M. R. Matthews, C. E. Wieman, and E. A. Cornell, *Science* **269**, 198 (1995).
 - [2] C. C. Bradley, C. A. Sackett, J. J. Tollett, and R. G. Hulet, *Phys. Rev. Lett.* **75**, 1687 (1995); C. C. Bradley, C. A. Sackett, and R. G. Hulet, *ibid.* **78**, 985 (1997).
 - [3] K. B. Davis, M. -O. Mewes, M. R. Andrews, N. J. van Druten, D. S. Durfee, D. M. Kurn, and W. Ketterle, *Phys. Rev. Lett.* **75**, 3969 (1995).
 - [4] D. G. Fried, T. C. Killian, L. Willmann, D. Landhuis, S. C. Moss, D. Kleppner, and T. J. Greytak, *Phys. Rev. Lett.* **81**, 3811 (1998).
 - [5] F. Pereira Dos Santos, J. Léonard, Junmin Wang, C. J. Barrelet, F. Perales, E. Rasel, C. S. Unnikrishnan, M. Leduc, and C. Cohen-Tannoudji, *Phys. Rev. Lett.* **86**, 3459 (2001); A. Robert, O. Sirjean, A. Browaeys, J. Poupard, S. Nowak, D. Boiron, C. I. Westbrook, A. Aspect, *Science* **292**, 461 (2001).
 - [6] W. Ketterle and N. J. van Druten, in *Advances in Atomic, Molecular, and Optical Physics*, edited by B. Bederson and H. Walther (Academic, New York, 1996), Vol. 37, p. 181.
 - [7] O. J. Luiten, M. W. Reynolds, and J. T. M. Walraven, *Phys. Rev. A* **53**, 381 (1996).

- [8] E. A. Burt, R. W. Ghrist, C. J. Myatt, M. J. Holland, E. A. Cornell, and C. E. Wieman, Phys. Rev. Lett. **79**, 337 (1997); J. Söding, D. Guéry-Odelin, P. Desbiolles, F. Chevy, H. Inamori, and J. Dalibard, Appl. Phys. B **69**, 257 (1999).
- [9] D. M. Stamper-Kurn, M. R. Andrews, A. P. Chikkatur, S. Inouye, H. -J. Miesner, J. Stenger, and W. Ketterle, Phys. Rev. Lett. **80**, 2027 (1998).
- [10] B. P. Anderson, P. C. Haljan, C. E. Wieman, and E. A. Cornell, Phys. Rev. Lett. **85**, 2857 (2000).
- [11] R. Onofrio, C. Raman, J. M. Vogels, J. R. Abo-Shaeer, A. P. Chikkatur, and W. Ketterle, Phys. Rev. Lett. **85**, 2228 (2000).
- [12] M. -O. Mewes, M. R. Andrews, D. M. Kurn, D. S. Durfee, C. G. Townsend, and W. Ketterle, Phys. Rev. Lett. **78**, 582 (1997); B. P. Anderson and M. A. Kasevich, Science **282**, 1686 (1998); E. W. Hagley, L. Deng, M. Kozuma, J. Wen, K. Helmerson, S. L. Rolston, and W. D. Phillips, Science **283**, 1706 (1999); I. Bloch, T. W. Hänsch, and T. Esslinger, Phys. Rev. Lett. **82**, 3008 (1999).
- [13] C. A. Sackett, C. C. Bradley, and R. G. Hulet, Phys. Rev. A **55**, 3797 (1997).
- [14] P. W. H. Pinkse, A. Mosk, M. Weidemüller, M. W. Reynolds, T. W. Hijmans, and J. T. M. Walraven, Phys. Rev. A **57**, 4747 (1998).
- [15] M. Yamashita, M. Koashi, and N. Imoto, Phys. Rev. A **59**, 2243 (1999); M. Yamashita, M. Koashi, Tetsuya Mukai, M. Mitsunaga, and N. Imoto, *ibid.* **62**, 033602 (2000).
- [16] In this paper, we adopt the opposite sign of the notations of evaporation rates $\dot{n}_{ev}(\mathbf{r})$ and $\dot{e}_{ev}(\mathbf{r})$ defined in Ref. [15].
- [17] Yu. Kagan, B. V. Svistunov, and G. V. Shlyapnikov, Pis'ma Zh. Eksp. Teor. Fiz. **42**, 169 (1985) [JETP Lett. **42**, 209 (1985)].
- [18] K. Berg-Sørensen, Phys. Rev. A **55**, 1281 (1997); **56**, 3308 (E) (1997).
- [19] Y. Torii, Ph.D. thesis, University of Tokyo, 2000 (unpublished).
- [20] H. Wu, E. Arimondo, and C. J. Foot, Phys. Rev. A. **56**, 560 (1997).
- [21] Y. Yoshikawa, K. Araki, T. Kuwamoto, and T. Hirano (private communication).